Supporting Information

Wang et al. 10.1073/pnas.0909479107

SI Methods

Vα14-Vβ8.2 TCR Refolding. Because initial refolding of the Vα14/Vβ8.2 TCR resulted in increased αα-homodimerization, we designed a construct in which the Vα14 (TRAV11*02, TRAJ18*01; CDR3α: CVVGDRGSALGRLHF) and Vβ8.2 chains (TRBV13-2*01, TRBJ2-5*01, TRBD2*01; CDR3β: CASGEGGLGGPTQYF) were cloned upstream of the human TCR α and β constant domains, respectively. To avoid introducing an additional restriction site between variable and constant domains, we used an internal *Bgl*II site within the constant domain of the β chain (in pET30a), and the variable α chain was fused to a *BamH*I site within the human constant domain (in pET22b$^+$) that was created as a silent mutation through site-directed mutagenesis (5′-CCT GAC CCT-3′ changed to 5′-CC**G** GA**T** CCT-3′). In addition, two cysteines were incorporated in the constant domain (TRAC 48 and TRBC 57) to form a disulfide bond, and a free cysteine in the constant TCRβ chain was mutated to serine, to facilitate refolding (1). Both α and β chains were expressed separately in BL21 (DE3) cells, and inclusion bodies were purified using standard methods. Inclusion bodies were dissolved in 50 mM Tris-HCl, 5 mM EDTA, 2 mM DTT, and 6 M guanidine-HCl, pH 7.0, and stored at −80 °C. The TCR was refolded essentially as reported for the human Vα24Vβ11 TCR (2, 3) with the following modifications: 32 mg of α chain and 48 mg of β chain were thawed, mixed, and pulsed with 1 mM DTT and then added drop-wise to 1 L refolding buffer (50 mM Tris-HCl, 0.4 M L-arginine, 5 M urea, 2 mM EDTA, 5 mM reduced glutathione, 0.5 mM oxidized glutathione, and 0.2 mM PMSF, pH8.0, at RT) under constant stirring at 4 °C. After 16 h, the same amount of α and β chains were added again, and stirring continued for an additional 8 h. The refolding mix was then dialyzed overnight against 18 L of 10 mM Tris-HCL, 0.1 M urea, and pH 8.0, and then again for 8 h against the same fresh buffer. Finally, the refolding mix was dialyzed against 18 L of 10 mM Tris-HCl, pH 8.0, for 24 h. The refolded protein was purified as outlined in the *Methods*.

BirA-Tagged Vα14-Vβ8.2 TCR Gene Construction. We amplified a C-terminal fragment of the human TCRβ constant domain with two synthetic oligonucleotides to include a birA-tag: 5′-GCAG*A-GATCT*CCCACACCC (an internal *Bgl*II site in the human TCRβ constant domain, in italics) and 5′-*GAATTC*TTA**ACGATGATTC-CACACCATTTTCTGTGCATCCAGAATATGATGCAG**TGCTCT ACCCCAGGCCTC (*Eco*RI site, italics; birA sequence in boldface type). The resulting DNA fragment was digested with *Bgl*II and *Eco*RI and ligated with *Bgl*II-*Eco*RI-digested pET30a containing the mouse Vβ8.2-human Cβ chimeric TCR.

Surface Plasmon Resonance Studies. Recombinant mCD1d protein containing a birA-tag (LHHILDAQKMVWNHR) between the CD1d ectodomain and C-terminal hexahistidine tag was expressed and purified as described previously (4). Before lipid loading, birA-tagged mCD1d was biotinylated using a commercial biotinylation kit (Avidity) and purified from free biotin by SEC on Superdex S200 10/300 GL. Glycolipids (dissolved in 0.5% Tween 20) were loaded overnight, and ≈1,000 RU of mCD1d was immobilized on a streptavidin sensor chip (Biacore). The TCR protein was diluted in running buffer without Tween 20 (10 mM Hepes, 150 mM NaCl, and 3 mM EDTA, pH 7.4) to prevent or slow down washing the glycolipid off mCD1d. A series of increasing concentrations of the TCR in duplicate were passed over the mCD1d glycolipid complex (0.01–0.64 μM for α-GalCer and 0.04–2.5 μM for GalA-GSL. The TCR was injected for a 3-min association for α-GalCer or 5-min association for GalA-GSL, and dissociation was continued over 30 min for α-GalCer or 5 min for GalA-GSL). Alternatively, the biotinylated TCR was immobilized up to 1,000 RU, and serial dilutions (0.14–36 μM) of mCD1d-BbGL-2c complexes were injected for a 2-min association and 2-min dissociation. Experiments were carried out at 25 °C with a flow rate of 30 μL/min and performed in total two or three times, each time with a different TCR preparation. Kinetic parameters were calculated after subtracting the response to mCD1d molecules that were incubated only with Tween 20, using a simple Langmuir 1:1 model in the BIA evaluation software version 4.1.

Data Collection and Crystal Structure Determination. Crystals were flash-cooled at 100 K in mother liquor containing 20% glycerol. Diffraction data from a single crystals were collected at the Stanford Synchrotron Radiation Laboratory (SSRL) beamlines 7.1 (mCD1d-BbGL-2c) and 9.2 (mCD1d-BbGL-2f) and were processed to 2.05 Å and 1.85 Å resolution, respectively with the Denzo-Scalepack suite (5). mCD1d-BbGL-2c crystallized in monoclinic spacegroup $P2_1$ (unit cell dimensions: a = 41.7 Å; b = 97.8 Å; c = 55.4 Å; β=107.0), and mCD1d-BbGL-2f crystallized in orthorombic spacegroup $P2_12_12_1$ (unit cell dimensions: a = 42.1; b = 110.4; c = 107.5).

In both crystals, one mCD1d-glycolipid molecule occupies the asymmetric unit with an estimated solvent content of 45.4% and V_m of 2.28 Å^3/Da for mCD1d-BbGL-2c) or 53.7% solvent content and V_m of 2.6 Å^3/Da for mCD1d-BbGL-2f. Molecular replacement was carried out in CCP4 (6) using the program MOLREP (7), with the protein coordinates from the mCD1d-sulfatide structure [PDB code 2AKR (4)] as the search model. For both crystal structures, rigid-body refinement was carried out, followed by several rounds of restrained refinement against the maximum likelihood target in REFMAC 5.2. The refinement progress was judged by monitoring the R_{free} for cross-validation (8). The model was rebuilt into σ_A-weighted, 2*Fo –Fc* and *Fo – Fc* difference electron density maps using the program COOT (9). Final refinement steps were performed using the TLS procedure in REFMAC (10) with three anisotropic domains (α1–α2 domain including carbohydrates and glycolipid, α3-domain, and β_2M). The mCD1d-BbGL-2c structure has a final R_{cryst} = 20.8% and R_{free} = 25.1%, whereas the mCD1d-BbGL-2f structure has a final R_{cryst} = 20.5% and R_{free} = 23.3%. The quality of both models (Table S1) was excellent, as assessed with the program Molprobity (11).

TCR Modeling. The structures of mCD1d in complex with either BbGL-2c or BbGl-2f were each superimposed onto the mCD1d portion of the recently determined crystal structure of the mCD1d-α-GalCer-Vα14Vβ8.2 TCR complex [PDB code 3HE6 (12)]. Under the assumption that the TCR maintains a conserved footprint onto CD1d, even when the *Borrelia* ligands are bound, the current TCR model illustrates the binding orientation of BbGL-2c and BbGL-2f within the CD1d-TCR complex.

1. Boulter JM, et al. (2003) Stable, soluble T-cell receptor molecules for crystallization and therapeutics. *Protein Eng* 16:707–711.
2. Gadola SD, et al. (2006) Structure and binding kinetics of three different human CD1d-α-galactosylceramide-specific T cell receptors. *J Exp Med* 203:699–710.
3. Kjer-Nielsen L, et al. (2006) A structural basis for selection and cross-species reactivity of the semi-invariant NKT cell receptor in CD1d/glycolipid recognition. *J Exp Med* 203:661–673.
4. Zajonc DM, et al. (2005) Structural basis for CD1d presentation of a sulfatide derived from myelin and its implications for autoimmunity. *J Exp Med* 202:1517–1526.

5. Otwinowski Z, Minor W (1997) HKL: Processing of X-ray diffraction data collected in oscillation mode. *Methods Enzymol* 276:307–326.
6. CCP4 (1994) Collaborative Computational Project, Number 4. The CCP4 Suite: Programs for protein crystallography. *Acta Crystallogr* D50:760–763.
7. Vagin AA, Teplyakov A (1997) MOLREP: An automated programm for molecular replacement. *J Appl Cryst* 30:1022–1025.
8. Brünger AT (1992) Free R value: A novel statistical quantity for assessing the accuracy of crystal structures. *Nature* 355:472–475.
9. Emsley P, Cowtan K (2004) Coot: Model-building tools for molecular graphics. *Acta Crystallogr D Biol Crystallogr* 602126–2132.
10. Winn MD, Isupov MN, Murshudov GN (2001) Use of TLS parameters to model anisotropic displacements in macromolecular refinement. *Acta Crystallogr* D57:122–133.
11. Lovell SC, et al. (2003) Structure validation by Calpha geometry: φ,ψ and Cbeta deviation. *Proteins* 50:437–450.
12. Pellicci DG, et al. (2009) Differential recognition of CD1d-α-galactosyl ceramide by the V β 8.2 and V β 7 semi-invariant NKT T cell receptors. *Immunity* 31:47–59.
13. Zajonc DM, et al. (2005) Structure and function of a potent agonist for the semi-invariant natural killer T cell receptor. *Nat Immunol* 8:810–818.
14. Koch M, et al. (2005) The crystal structure of human CD1d with and without α-galactosylceramide. *Nat Immunol* 8:819–826.

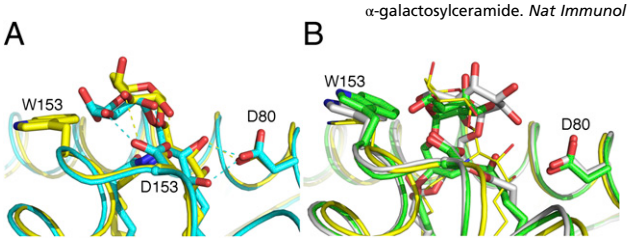

Fig. S1. Structural differences between mouse and human CD1d. (*A*) Overlay of human (yellow) and mouse (light blue) CD1d-α-GalCer complexes [PDB codes 1Z5L (13) and 1ZT4 (14)] illustrates the influence of tryptophan153 (W153) in the presentation of the galactose epitope. (*B*) Superimposition of the human CD1d-α-GalCer structure (yellow) with that of mouse CD1d with bound BbGL-2c (gray) and BbGL-2f (green). The influence of the mCD1dG155W mutant is modeled, and indicates that the tryptophan side chain is too close to the galactose moieties and will affect the presentation of both BbGL-2c and BbGL-2f.

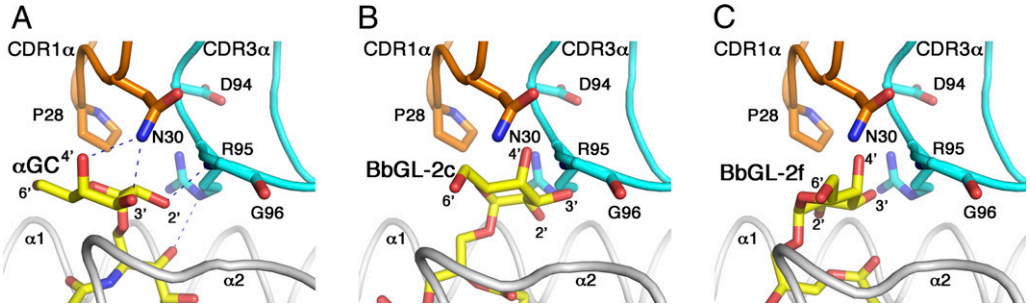

Fig. S2. TCR-glycolipid structures and models. (*A*) Crystal structure of the mCD1d-αGalCer-Vα14Vβ8.2 TCR complex [PDB code 3HE6 (12)] and derived models of mCD1d-bound BbGL-2c (*B*) and BbGL-2f (*C*). Note that this model illustrates the steric clashes between the *Borrelia* glycolipid BbGL-2c with CDR3α of the TCR in this docking orientation. H bonds are illustrated as blue dashed lanes only for only the actual crystal structure but not for the models. Glycolipids are depicted with yellow sticks, mCD1d in gray, TCR α chain CDR1 region in orange, and CDR3 region in cyan. TCR residues that interact with α-GalCer in *A* are shown as sticks.

Table S1. Data collection and refinement statistics

	mCD1d-BbGL-2c	mCD1d-BbGL-2f
Data collection		
Resolution range (Å)*	50.0–2.05 (2.12–2.05)	40.0–1.85 (1.92–1.85)
Completeness (%)*	93.3 (90.0)	91.2 (94.4)
Number of unique reflections	25,018	39,906
Redundancy	4.4	3.2
R_{sym}*[†] (%)	6.7 (60.4)	6.1 (38.3)
I/σ*	35.9 (3.6)	21.6 (3.6)
Refinement statistics		
Number of reflections (F > 0)	23,962	38,588
Maximum resolution (Å)	2.05	1.85
R_{cryst}[‡] (%)	20.8 (31.0)	20.5 (23.1)
R_{free}[§] (%)	25.1 (32.0)	23.3 (23.9)
Number of atoms	3,151	3,272
Protein	2,911	2,942
Glycolipid	53	55
N-linked carbohydrate	56	42
Solvent molecules (waters/DMSO)	131/0	229/4
Ramachandran statistics (%)		
Favored	98.6	98.6
Outliers	0.0	0.0
RMSD from ideal geometry		
Bond length (Å)	0.016	0.013
Bond angles (°)	1.70	1.43
Average B values (Å^2)[‖]		
Protein	52.5	25.6
Glycolipid	77.5	53.6
Water molecules	32.45	19.6
Carbohydrates	70.7	37.2

*Numbers in parentheses refer to highest-resolution shell.

[†]$R_{sym}=(\Sigma_h\Sigma_i|I_i(h)-\langle I(h)\rangle|(\Sigma_h\Sigma_i I_i(h))\times100$, where $\langle I(h)\rangle$ is the average intensity of i symmetry-related observations for reflections with Bragg index h.

[‡]$R_{cryst}=(\Sigma_{hkl}||F_o|-|F_c||/\Sigma_{hkl}|F_o|)\times100$, where F_o and F_c are the observed and calculated structure factors, respectively, for all data.

[§]R_{free} was calculated as for R_{cryst}, but on 2% (CD1d) and 1.5% (TCR) of data excluded before refinement.

[‖]B values were calculated with the CCP4 program TLSANL (1).

1. Winn MD, Isupov MN, Murshudov GN (2001) Use of TLS parameters to model anisotropic displacements in macromolecular refinement. *Acta Crystallogr* D57:122–133.